623

May 4, 1979

PROPOSAL TO STUDY HIGH MASS STATES DECAYING INTO $\phi^o\pi^\pm$ AND $\phi^o\phi^o$ PRODUCED CENTRALLY IN 300 GeV/c π^-p INTERACTIONS

R. Abrams, R. Ahrens, J. Albright, G. Collins, F. T. Dao, R. Diamond, H. Fenker, J. Ficenec, H. Goldberg, D. Green*, S. Hagopian, V. Hagopian, C. Halliwell, D. Harmer, E. Jenkins, R. Kalbach, K-W Lai*, T. P. Lang, J. Lannutti, Z. Ming Ma. W. A. Mann, S. Margulies, J. Marrafino, D. McLeod, A. Napier, A. Pifer, J. Poirier, S. Revcroft, C. Roos, J. Schneps, J. Solomon, W. Trower, J. Waters, M. Webster, W. Orance, R.Siegel

Arizona, Brookhaven National Laboratory, Chicago Circle, Fermilab, Florida State, Georgia Tech, Michigan State, Notre Dame, Tufts, Vanderbilt, V.P.I., William and Mary Collaboration

*Co-Spokesmen
840-3104
666-3864

SUMMARY

We propose to use a 300 GeV/c π^- beam incident on an upgraded Fermilab MPS to search for new massive states decaying into the virtually unexplored $\phi^o\pi^\pm$ and $\phi^o\phi^o$ final states. The $\phi^o\pi^\pm$ system is a baryonium and weak decay filter, while the $\phi^o\phi^o$ system selects $(\bar{q}q)_{C=+1}$ states which are inaccessible to e^+e^- experiments.

The $\phi^o\pi^\pm$ system could reveal:

a. Charm, $F^\pm(c\bar{s})$, to a level $\sigma B \sim 40$ nb

b. I = 1 vector mesons with OZI violating decays to a level $\sigma B \sim 3$ nb for 4 GeV/c^2 mass

c. Exotic mesons consisting of four quarks.

The $\phi^o\phi^o$ system could reveal:

a. $\eta_c \to \phi^o\phi^o$ to a level $\sigma B \sim 8$ nb

b. We intend to explore the high-mass region for $\eta_b \to \phi^o\phi^o$. The production cross section can be estimated to be $\sim$ 10 nb.

The MPS aperture is large enough to provide good geometric efficiency for masses up to 10 GeV/c^2 in the restricted region $y^* \simeq 0$ where production is expected to be concentrated.

We request 1000 hours total testing and data-taking time. The data triggers will be ϕ^o, $\phi^o\pi^\pm$, and $\phi^o\phi^o$.

A. Introduction

We propose to use a trigger scheme which utilizes the unusual topological features of high mass $\phi^o\pi^\pm$ and $\phi^o\phi^o$ states. The $\phi^o\pi^\pm$ system serves to filter out the great majority of inclusive hadronic interactions at high energy. Requiring a ϕ^o reduces the hadronic background by a factor of roughly 75. In addition, high mass states decaying via the two-body $\phi^o\pi^\pm$ mode impart substantial transverse momentum to the pion. The additional requirement of pion transverse momentum $\geq$ 900 MeV/c results in an overall reduction factor of about 400 with respect to the peripheral inclusive hadronic background. This filter allows for a sensitive search for new high mass states at the cross section times branching ratio level σB of roughly 40 nb for $M \geq 2$ GeV/c^2.

The $\phi^o\pi^\pm$ system is an OZI forbidden final state for the strong decay of any quark-antiquark ($\bar{q}q$) meson.[1] Thus, the existence of an $\phi^o\pi^\pm$ decay mode indicates either an OZI violating strong decay, a weak decay (e.g., $F^\pm \rightarrow \phi^o\pi^\pm$), or an allowed decay of a multiquark state (e.g., $\bar{q}^2q^2$ I = 1 baryonium states). Hence, the large hadronic filter factor passes very interesting types of decays with greatly improved signal-to-noise ratio.

The decay mode $\phi^o\phi^o$ is a filter for $(\bar{q}q)_{C=+1}$ states with $q = s,c,b \ldots$[1]. Such states are inaccessible to e^+e^- experi-

ments. The sensitivity which can be achieved is comparable to that from the only previously published measurement[2]. Given that the measurement was at low energy in an exclusive channel while this experiment is inclusive at Fermilab, one can improve on the existing data set by two orders of magnitude.

One expects that high mass states which are produced in pairs, such as $F\bar{F}$, are produced centrally[3], that is nearly at rest in the CM system ($y^* = 0$) with a width in rapidity which is rather small. Thus, it is crucial to have good geometrical acceptance for the kinematic region $y^* \approx 0$. In addition, heavier states are produced with larger transverse momentum (p_t) than pions, and their two-body decays contribute additional p_t. The large production and decay angles necessitate a large aperture system such as the MPS (see Figure 3).

Previous studies of ϕ^o production at Fermilab energies have been made with relatively small aperture systems or via the $\mu^+\mu^-$ mode. By using a large aperture system one can study the dynamics of ϕ^o production. For example, is the hidden strangeness of the ϕ^o compensated for, and if so, is it locally or globally compensated[4]?

One can estimate[3] that $\geq$ 50% of all F come from F*, and that the only allowed decay is $F^* \rightarrow F\gamma$. Utilizing the large calorimeter available at the MPS, one can improve on the sensitivity

to the F by roughly a factor of two. This improvement is due to three factors: two narrow state mass plot cuts, good geometric efficiency to detect the γ, and good efficiency to detect the other γ from $\pi^o \rightarrow \gamma\gamma$ decay leaving only single photons. Hence, neutral particle detection will be very useful.

Most of the apparatus for this experiment already exists at the Fermilab MPS in the M6W beam. The addition of a few rather coarse grained drift chamber planes would finish the conversion of the MPS into a 10,000 PWC wire plus drift chamber system with high rate capability. Two finely segmented Cerenkov counters allow for unambiguous identification of kaon pairs.

The scale of unwanted background is set by $\sigma_I \simeq 20$ mb, $\langle n_{\pi^\pm} \rangle \simeq 8$. The existence of a charged kaon pair in itself does not provide a very substantial reduction factor, $\sigma(K^+K^-) \simeq 5$ mb. However, ϕ^o production is a small fraction of $\sigma(K^+K^-)$[5,6], $\sigma(\phi^o \rightarrow K^+K^-)/\sigma(K^+K^-) \sim 1/20$.

A crude pretrigger ($\sigma \sim 600$ μb) will select a ϕ^o on the basis of low Q value ($p_K^* =$ CM momentum = 128 MeV/c) which implies a small space angle. The MPS would be converted into a spectrometer that would indeed deal with multiparticle systems by utilizing sophisticated trigger electronics developed at Fermilab[7]. A tight selection using five MPS PWC planes as a stand-alone smart trigger system would constitute a final trigger ($\sigma \sim 15$ μb).

Requiring a pion with p_t >900 MeV/c causes only a minor loss of events for high mass, M $\geq$2.25 GeV/c^2, states decaying into $\phi^o\pi^\pm$. Given that the background is peripheral, $\langle p_t \rangle$ ~330 MeV/c, this requirement provides an additional reduction factor of roughly 5 in trigger rate. The resulting trigger cross section implies that in a 500 hour run a sensitivity at least an order of magnitude better than that from existing data would be achieved.

B. Experimental Layout

1. Beam

The beam will be the M6W beam set for negatives at 300 GeV/c using the existing beam line counters. Beam requirements are modest; using a 5 cm thick Be target, a 5 mm spot size and a few $10^6 \pi^-$/spill are sufficient.

2. Upstream Arm and MPS Magnet

The MPS has been described elsewhere[8]. Basically, it is a 10,000 wire PWC system giving charged particle tracking for $\theta_x \leq$160 mrad and $\theta_y \leq$110 mrad, with a transverse momentum kick of 600 MeV/c provided by a superconducting 48D48 magnet.

A schematic plan view of the apparatus is shown in Figure 1. The incident beam is tracked in two PWC modules which are not shown. Wide angle charged recoils are detected via current division readout of a cylindrical PWC

with axial wires. Wide angle neutral tracks are tagged in a series of lead-scintillator sandwich counters.

Small angle, charged particles are detected first in the upstream arm of the MPS, consisting of ~5,000 wires. The planes are x, x, u, v, y, y (A); u, v, (B"); x (B´); x, y (B); and x, y, (C). Production angles are measured to an accuracy of $d\theta_x = \pm .25$ mrad and $d\theta_y = \pm .34$ mrad.

The MPS magnet aperture is lined with cathode strip chambers to determine the momentum of slow secondaries which are swept away (γ_A, γ_B).

3. Downstream Arm

The downstream arm consists of another roughly 5,000 PWC wires x, u, y, v, x (D, D´). At present these chambers are followed by 8 spark chamber modules and small PWC planes x, u, v, x (F). A reasonable upgrade to higher beam rates would entail the construction of four planes of drift chamber, x, u, y, x (DR). Outgoing angles are then measured rather well, $d\theta'_x = 0.1$ mrad, in the bend (x, z) plane. Hence, momenta are measured to $dp = \pm\, p^2(4.7 \times 10^{-4}\ \mathrm{GeV/c^{-1}})$. Typical trajectories for $\pi^- p \to M^+ X$, $M^+ \to \phi^o \pi^+$, $\phi^o \to K^+ K^-$, $M = 4\ \mathrm{GeV/c^2}$ are also shown in Figure 1.

4. Cerenkov Counters

Mass identification of forward tracks is provided by two segmented Cerenkov counters, one with 24 cells ($\check{C}_A$) and one with 32 cells ($\check{C}_B$). $\check{C}_A$ will be filled with air and $\check{C}_B$ with helium. The pion thresholds are 5.75 GeV/c and 15.0 GeV/c, respectively, while the kaon thresholds are 20.5 GeV/c and 53.6 GeV/c. These thresholds are well matched to the kinematics of central production as will be discussed later.

5. Calorimeter

Neutral particle position is determined by cathode strip PWC. Particle energy is measured by a fine grained lead-steel calorimeter which subtends the magnet aperture solid angle.

C. Geometric Acceptance

Inclusive background was generated using the model of ref. 3 which incorporates the general features of inclusive production; $\langle p_t \rangle$ increases with secondary mass, and production is more central as the secondary mass increases.

$$E \frac{d\sigma}{d\vec{p}} = \frac{A}{(M_t + B)^C} \; e^{-D/(y^*_{max} - y^*)} E e^{-p_t}$$

where $M_t = \sqrt{p_t^{\,2} + M^2}$

and y^*_{max} = maximum rapidity for a given M in the CM frame.

Background was assumed to be uncorrelated and all particles decayed isotropically. The geometric efficiencies for background were found to be: $\varepsilon_K = .78$, $\varepsilon_\pi = .62$, $\varepsilon_{KK\pi} \equiv \varepsilon_K^2 \varepsilon_\pi = .38$ and $\varepsilon_\phi = .72$, $\varepsilon_{\phi\pi} \equiv \varepsilon_\phi \varepsilon_\pi = .45$. The calorimeter aperture provides a good match to the magnet aperture.

The $\phi^o \pi^\pm$ signal was generated using the same form for the cross section and assuming local compensation of quantum number, i.e., $M \simeq 2\ M_{\phi\pi}$. The resulting geometric efficiency to detect all decay products ($K^+K^-\pi^\pm$) is shown in Figure 2. In Figure 2a one sees that the acceptance is a weak function of mass, typically $\varepsilon_M \simeq 0.6$. In Figures 2c and 2d are shown the acceptances as a function of laboratory rapidity for 2.0 and 5.0 GeV/c^2 masses, respectively. Clearly the large aperture of the MPS yields good acceptance, typically $\varepsilon_M \sim 0.5$, for $y^* = 0$. Note that if the production distribution is not as central as was assumed, the quoted acceptance will be a lower limit since $\varepsilon_M \to 1$ rapidly as y_M increases.

In Figure 2b is shown the probability that the $\pi^\pm$ from the $\phi^o \pi^\pm$ decay will have $p_{t\pi\pm} > 900$ MeV/c. Since the background is peripheral, $d\sigma/dp_t^2 \alpha e^{-bp_t}$, $\langle p_t \rangle = 2/b \sim 330$ MeV/c, $\varepsilon(p_t > p_{t_{min}}) = (1 + bp_{t_{min}})e^{-bp_{t_{min}}} \simeq .03$, while the two-body decay results in large p_t, this cut provides a useful background discrimination. The probability rises rapidly with M and is ≥ 0.8 for $M \geq 3$ GeV/c^2.

D. Triggering

1. Pretrigger

Previously the MPS has been triggered either externally using a calorimeter or internally using hit multiplicity in the PWC planes. It is proposed to expand the trigger capability of the MPS to encompass modern complex fast logic decisions[7].

The trigger scheme will utilize the unusual topological features of high mass $\phi^o\pi^\pm$ states. Typical (θ_x, θ_y) plots for M =2, 5 GeV/c^2 are shown in Figure 3. The parent particle is shown with $p_t = \langle p_t \rangle = .9$, 1.3 GeV/c and $y_M = \langle y_M \rangle$ for M = 2,5 GeV/c^2, respectively. Subsequent sequential decays with $\theta^* = 90^o$ at all ϕ^* are also shown. Note that the K^+K^- pair has a small opening angle in all cases. Note also that the $\phi^o\pi^\pm$ coplanarity is not totally washed out by the large production p_t of the parent particle. These two general features are confirmed by detailed Monte Carlo calculations. For example, Monte Carlo distributions, for M = 4 GeV/c^2, of θ_K and $\theta_{K^+K^-}$ are shown in Figures 4a and 4b, respectively.

A pretrigger utilizing standard fast logic will be used to reduce the number of events to be processed. The ingredients are an x plane of PWC (C) whose wires are "ORED" into a variable width 32 element fast stand-along hodoscope and the $\check{C}_A$ Cerenkov, 12 cells across horizontally. These cells are also of varying size in order to match the

inclusive particle angular distribution. The pretrigger would require two tracks within a hodoscope element which matchs one of the Cerenkov cells. The associated Cerenkov cell will be required in veto.

The pretrigger corresponds to an inelastic event with two tracks of small opening angle, $|\theta_{x1} - \theta_{x2}|<40$ mrad. These tracks are pions with momenta <5.75 GeV/c or kaons <20.5 GeV/c or protons (negligible) <38.7 GeV/c. As given in Table I an estimate of the pretrigger cross section gives 600 μb.

Inelastic reactions will be selected by requiring an outscatter from a beam veto counter located downstream of the MPS magnet. For 5×10^5 π^-/spill incident on a 5 cm Be target, the inelastic rate is 65,000 interactions/sec. The pretrigger cross section of 600 μb corresponds to a rate of ~1700 pretriggers/sec. Hence, a 50 μsec high level trigger decision time will only result in a 10% deadtime loss. Clearly, an error of a factor of two in the pretrigger rate will not change the ultimate sensitivity appreciably.

2. High Level Trigger

The high level trigger has 50 microseconds to decide if the pretrigger event was acceptable. First, the hits in five planes will be encoded and stacked into a memory Bx,

Bu, Bv, Dx, Dx'. The B planes will be rotated at $\pm 120^{\circ}$ angles yielding the simple algorithm for a track, $Bx_i + Bu_j + Bv_k = 0$. Each i and j pair will be checked for a valid k using the FNAL track finder subsystem[7]. Valid triples will be stored in a stack.

Simultaneous with the $(\theta_{xi}, \theta_{yi})$ determination of a track, momentum will be calculated. Since the 5 cm Be target is an effective fourth point on the track, the track finder subsystem can again be used. Related track segments upstream and downstream of the magnet should intersect at the magnet centerline. This requirement leads to a linear algorithm, $aBx_i = bDx_j + D'x_k$. For valid matched track segments the charge (q) and momentum (p) of the track will be computed and stored in a stack, $(1/pq_i) = c(Dx_i' - Dx_i) + d\ Bx_i$.

The logic modules to do threefold coincidence track finding have already been developed and tested at Fermilab. The MPS PWC data which is latched into shift registers by the pretrigger will be immediately extracted and encoded for the five planes. This encoding is experiment dependent. However, beyond that level the logic is essentially experiment independent and can be thought of as an extension of standard NIM logic.

The two track finding loops will yield (p, q, θ, φ) for each track. The two pretrigger tracks will have their mass calculated as $M_{KK}^2 \simeq 4\ M_K^2 + p_1 p_2 \left[(x_1 - x_2)^2 + (y_1 - y_2)^2\right]/L^2$ after first checking that $q_1 q_2 < 0$. A cut on $M_{KK} = M_\phi$ will be applied. All other tracks will be searched through for $p_t^2 = p_i^2 \left[(x_i^2 + y_i^2)/L^2\right]$ picking the maximum. The maximum track must have $p_t^2 \geq 0.8\ (\mathrm{GeV/c})^2$. The efficiency of this cut for desired events is shown in Figure 2b; it ranges from ~25% at M = 2 GeV/c^2 to ~100% at M = 5 GeV/c^2. Finally, noting from Figure 3 that $\phi^o - \pi^\pm$ coplanarity is not completely washed out by the parent p_t, it will be required that $|(\phi_{K1} + \phi_{K2})/2 - \phi_\pi| > \pi/2$. Taken together we calculate a factor of 8 reduction in trigger cross section. Tighter cuts will be delayed until offline analysis. The efficiency of these cuts for desired events varies with M from 0.2 to 0.9 for M = 2 to 5 GeV/c^2, respectively.

The probability per pion to have $p_{t\pi} > 0.9$ GeV/c was determined by Monte Carlo methods to be .05. Since $\langle n_{\pi\pm}\rangle \sim 8$ and $\varepsilon_\pi = .63$ the probability per inelastic event to have a high p_t pion is 0.25. Since the ϕ^o and $\pi^\pm$ are assumed to be uncorrelated, the coplanarity cut removes ½ of all combinations. Thus, the high level trigger reduces the pretrigger events by a factor of ~40 down to 15 μb. This trigger rate is sufficiently low, $\sigma_{trig}/\sigma_I \simeq 1/1300$, as to provide for a sensitive search for rarely produced states.

E. Data Rates, Sensitivity

The pretrigger rate of 1700 pretriggers/sec is reduced by fast decision logic to a final trigger rate of 40 events/spill. In a 500 hour run a total of 7.2 million triggers will be taken, with 480 events corresponding to 1 nb of trigger rate.

Monte Carlo results for the uncorrelated $\phi\pi$ mass distribution are given in Figure 4. In Figure 4c is shown the $\phi\pi$ inclusive mass distribution for events passing the geometric apertures and the pretrigger cuts. The $\phi\pi$ mass distribution is shown in Figure 4d for events which pass the final trigger cuts. Clearly, the main effect of the final trigger is to put a low mass cut on the $\phi\pi$ mass by requiring $M \gtrsim 2.0$ GeV/c^2. The fraction of inclusive background within a 100 Mev/c^2 mass slice is ~9%/100 Mev/c^2 for $M = 2$ GeV/c^2 and $\leq$.3%/100 Mev/c^2 for $M \geq 4$ GeV/c^2.

Clearly, mass resolution is crucial. Assuming decays in the (x,z) plane (worst case), $M \gg M_\phi$, M_π, and symmetric decays one has:

$$M^2 = M_\phi{}^2(1 + p_\pi/p_\phi) + M_\pi{}^2(1 + p_\phi/p_\pi) + p_\pi p_\phi(\theta_{x\phi} - \theta_{x\pi})^2$$

$$dM = \frac{2\sqrt{2}}{M} \sqrt{(p\theta^2 dp)^2 + (p^2\theta d\theta)^2}, \quad p_\pi = p_\phi = p, \quad \theta_{x\phi} = -\theta_{x\pi} = \theta$$

Since the downstream angles are well measured, $d\theta \sim (\Delta p_t)dp/p^2$ where Δp_t is the MPS magnet p_t kick. Since $p_t = p\theta \sim M/2$

$$dM \sim \frac{MP}{\sqrt{2}}\left[\sqrt{\left(\frac{1}{\Delta p_t}\right)^2 + \left(\frac{1}{M/2}\right)^2}\right] d\theta_x$$

Evaluating this expression using $d\theta_x$ as given previously and p = the average value of the pion momentum through the apparatus as given by Monte Carlo results, one obtains dM = ±15 MeV/c^2, ±45 MeV/c^2 for M = 2, 4 GeV/c^2. Note that this result is a lower limit since the tracks will be 1-C fits to momenta, the $K^+ - K^-$ trajectories can be forced to have the ϕ^o mass, and all trajectories can be constrained to have a common vertex. All of these constraints will reduce the errors on the trajectories.

We assume also the uncorrelated mass plots given in Figure 4. Note that this is a lower limit since dynamical correlations are known to be short range, i.e., low mass. Note also that since $dp \alpha p^2$ one obtains a better result for the momentum by measuring the two kaons, $dp_K \sim dp_\phi/4$, rather than assuming that the ϕ^o is measured as a single particle as was done above in estimating dM. Within ±dM of M = 2, 4 GeV/c^2 there is a cross section of 400 nb, 40 nb. In 500 hours, this corresponds to 192 K, 12.2 K events. A 4σ bump corresponds to σB = 40, 3.2 nb. Suppose $B(M^\pm \to \phi^o\pi^\pm \hookrightarrow K^+K^-$ ~.04) then σ>1.0, .08 μb for M = 2, ≥4 GeV/c^2 would be detected as a 4σ bump. These are the limits for a single mass plot resonance search over the entire range of parent mass M. We will search for narrow enhancements, with good acceptance from 2 GeV/c^2 to 10 GeV/c^2, in the $\phi^o\pi^\pm$

mass plot with a cross section sensitivity of 1 μb for M = 2.0 GeV/c^2 to better than 100 nb for $M \geq 4.0$ GeV/c^2 assuming B = .04.

F. Search for Massive States

1. Single $\phi^o\pi^\pm$ Mass Plot

For the single $\phi^o\pi^\pm$ mass plot one obtains a 4σ sensitivity of σB = 40 nb at the $F^\pm$ mass. A reasonable branching ratio estimate for $B(F^\pm \to K^+K^-\pi^\pm)$ is ~4%[9] using a constant matrix element model. In this case the limit for a four standard deviation enhancement would be $\sigma_F \geq 1$ μb.

It is difficult to evaluate precisely how stringent a limit this might be. Previous searches using hadronic mass plots in $K^\pm\pi^\mp$ were limited by uncorrelated hadronic overlap to $\sigma_D \geq 40$ μb[10]. By utilizing the small ϕ^o production cross section that limit would be improved upon by an order of magnitude.

Some beam dump results observing single muons[11a] and prompt neutrinos[11b, c] give estimates of σ_{charm} ~10, 100 μb. Other experiments indicate that the central region is the source of anomalous events, e.g., the μ/π ratio rises rapidly as $y^* \to 0$. Data on $\mu^\pm e^\mp$ indicates that σ_{charm} ~20 μb. Finally, data on the production of ρ, f, g, and K^* (1420) using the model of Ref. 3 extrapolated to the D mass implies $\sigma_{charm} \sim 10$ μb[12]. These data lead one to believe

that charm is centrally produced with a cross section of at least 10 μb.

In the model of Ref. 3, $\sigma \alpha y^{*}_{max}{}^{2}\, e^{-D/y^{*E}_{max}} \left(\frac{M}{(M+B)}^{C}\right)$, where M is the minimum composite mass needed to locally conserve quantum numbers. In Figure 5 is plotted σ vs M for some measured particle yields and a conservative extrapolation to the charm systems. This extrapolation yields $\sigma_D \sim 7$ μb and $\sigma_F \sim 2$ μb assuming all D^* yield a D and all F^* yield an F. Note that this extrapolation is conservative in that the yields of K, $\bar{p}$, ϕ, and ψ are about an order of magnitude above the prediction. Note that without local compensation $\sigma_F \sim \sigma_D$. Thus, the single $\phi^o \pi^{\pm}$ mass search has by itself a reasonable probability of finding the F meson in hadronic interactions.

2. $F^* \rightarrow F\gamma$ Search, Double Mass Plot

A comfortable increase in sensitivity can be obtained by detecting photons associated with the F itself. The SU(4) mass relations $M_D{}^2 - M_\pi{}^2 = M_F{}^2 - M_K{}^2$ and $M_{D^*}^2 - M_\rho{}^2 = M_{F^*}{}^2 - M^2_{K^*}$ imply $M_F = 1926$ MeV/c^2, $M_{F^*} = 2056$ MeV/c^2. Since both F and F^* are isoscalar, $F^* \not\rightarrow F\pi$. Decays like $F^* \rightarrow F\eta$, DK are impossible by ≥ 300 MeV/c^2. Hence, one expects a narrow F^* with roughly 100 % branching ratio to $F^{\pm}\gamma$.

Since $M_{F^*} - M_F \simeq 130$ MeV, one expects[3] that a substantial

fraction of the F arise as decay products of the F^*. Using the graph in Figure 5 one would estimate roughly 75%. Thus, 50% is a reasonably conservative estimate. In Figure 6 is shown θ_γ vs p_γ for $y_F{}^* = 3.0$ and 4.0. The photon angles are substantial indicating that a large aperture calorimeter is needed for efficient detection. The indicated efficiency is ≥ 0.5 for detecting the photon accompanying the F.

Also indicated in Figure 6 is the expected mass resolution of the $F\gamma$ system due to momentum and angle errors. Clearly, a 15 MeV/c^2 bin would contain all the F^* signal. A single photon, unaccompanied by any other photon with $M_{\gamma\gamma} \simeq M_{\pi^o}$, with a mass $M_{F\gamma}$ within ±7 MeV/c^2 of the F^* mass will be required. The large calorimeter aperture is also an aid in removing photons from π^o decays, thus reducing combinatorial backgrounds.

The requirement of $M_{F\gamma} = M_F{}^* \pm 7$ MeV/c^2 leads to a roughly 50 fold reduction in background. Assuming half of all F come from F^* and $\varepsilon_\gamma = 0.5$ leads to a 4σ sensitivity of $\sigma B > 23$ nb or $\sigma > 0.57$ μb. This result is a factor of two improvement in sensitivity over the single mass plot $\phi^o\pi^\pm$ search.

3. $\phi^o\phi^o$ Mass Search

As seen in Figure 5, a conservative estimate of σ_{η_c} is

~7 μb. At lower energies in an exclusive reaction σ_{η_c} ~60 nb has been reported[13]. Given that there is a large increase of σ_ψ with $\sqrt{s}$ and that there is a large increase expected in going to an inclusive search, the above estimate seems plausible.

The pretrigger essentially requires a low mass KK pair. Using encoded Cerenkov information one can require two ϕ^o's in the final state with the high level trigger. The expected trigger rate of 2.5 μb is small with respect to the main $\phi^o\pi^\pm$ trigger.

The inclusive $\phi^o\phi^o$ mass distribution looks rather like the $\phi^o\pi^\pm$ mass distribution in Figure 4c with a suitable shift in mass origin. The sensitivity is indicated in Table I. Of the 2500 nb trigger, 28 nb is within ± dM of the η_c mass. Thus, a 4σ bump corresponds to σ_{η_c} $B(\eta_c \to \phi^o\phi^o)$ = 8 nb. Assuming σ_{η_c} is ~7 μb then the η_c will be observed in this experiment if $B(\eta_c \to \phi^o\phi^o) \geq 10^{-3}$.

Clearly, the sensitivity improves dramatically with mass just as in the case of the $\phi^o\pi^\pm$ single mass plot resonance search. Also, the apparatus has a large geometric acceptance out to 10 GeV/c^2 mass. We will try to partition the data into low mass (flux ~5 x 10^5/spill) and high mass (flux ~5 x 10^6/

spill). High mass data will have a raw sensitivity of ~5000 events/nb. Since the background level is unclear, no estimate of the η_b sensitivity is made.

4. Future Applications

We believe strongly that the technique of using sophisticated high level trigger logic has many applications in searches for rare high mass states. When the Tevatron becomes a reality, for example, experiments to search for hadronic production of beauty will become rather more feasible.[14] At 800 GeV/c using a π^- beam would take advantage of the presumed rise in $\bar{B}B$ cross section with $\sqrt{s}$ and the fact that pions are much more efficient at producing $\bar{B}B$ than protons. A crude estimate of the cross section is $\sigma(\pi^- p \rightarrow \bar{B}BX)$ ~0.7 μb.

The basic decay is expected to be $b \rightarrow c \rightarrow s$, so that for example the decay sequence $B^o \rightarrow D^+\pi^-$ followed by $D^+ \rightarrow K^- (n\pi)^{++}$ should exist. In this case, with M_B ~5 GeV/c^2, the topology of large $p_{t\pi}$ ~M/2 ~ 2.5 GeV/c with an additional kaon will provide very good discrimination against general hadronic background. Clearly, this example indicates that the proposed experimental technique will apply to several interesting experiments.

TABLE I

Requirement	Background		Effect	
None	σ_I = 20 mb		σB	
Pretrigger: 2 tracks $\bar{C}_A$ with opening angle <40 mrad	600 μb		.4σB	
High Level Trigger: M_{KK}, cut $p_{t\pi}$ >.9 GeV/c $\lvert\phi_\phi - \phi_\pi\rvert > \pi/2$	15 μb		M = 2 GeV/c^2 .09σB	M≥4 GeV/c^2 .36σB
$\phi\pi$ mass plot within ±dM of M 4σ effect	M = 2 GeV/c^2 400 nb	M≥4 GeV/c^2 40 nb	σB>40 nb	σB>3.2 nb
$\phi\pi\gamma$ mass plot within ±dM of F^* 4σ effect	8 nb		.022σB σB>23 nb	
High Level Trigger: M_{KK} cut, M_{KK} cut	2.5 μb		M≥2.8 GeV/c^2 .13σB	
$\phi\phi$mass plot within ±dM of M 4σ effect	28 nb		σB≥8 nb	

REFERENCES

1. J. J. Lipkin "Theoretical Review of Strange and Non-Strange Mesons", Experimental Meson Spectroscopy, Boston (1979)

2. A. Etkin, et al., Phys. Rev. Lett., 40 422 (1978)

3. M. Bourquin and J.-M. Gailliard, Nuc. Phys. 114B, 334 (1976)

4. Some conflicting evidence at lower energies has been presented

   a. V. Blobel, et al., Phys. Lett. 59B, 88 (1975)
   b. P. L. Woodworth, et al., Phys. Lett. 65B, 89 (1976)
   c. B. Ghidini, et al., Phys. Lett. 68B, 186 (1977)

5. K. J. Anderson, et al., Phys. Rev. Lett. 37, 799 (1976)

6. C. W. Akerloff, et al., Phys. Rev. Lett. 39, 861 (1977)

7. E. Barsotti, et al., Fermilab TM-823

8. "Multiparticle Spectrometer at Fermilab" prepared for MPS Workshop, March 4, 1977

9. C. Quigg and J. L. Rosner, Phys. Rev. D17, 239 (1978)

10. a. R. Lipton, et al., Phys. Rev. Lett., 40, 608 (1978)
    b. D. Bintinger, et al., Phys. Rev. Lett., 37, 732 (1976)

11. New Results in High Energy Physics - 1978 (Vanderbilt Conference) A.I.P. Proceedings #45 Edited by R. S. Panvini and S. E. Csorna

    a. B. Barish, et al.
    b. J. H. Mulvey, et al.
    c. T. Hansl, et al.
    d. A. G. Clark, et al.

12. G. Van Dalen, et al., Phys. Rev. Lett., 41, 176 (1978)

13. W. D. Apel, et al., Phys. Lett. 72B, 500 (1979)

14. D. R. Green, "Hadronic Production of Beauty at Tevatron Energies", Fermilab TM-830

FIGURE CAPTIONS

1. Schematic plan view of the MPS. Typical particle trajectories for $\pi^- p \to MX$, $M = 4$ GeV/c^2, $p_{tM} = 0.$ GeV/c, $y_M^* = 0.$ Decays $M \to \phi^o \pi^\pm$, $\phi^o \to K^+K^-$ are in the (x,z) plane with $\theta^* = 90^o$.

2. a. Geometric efficiency to detect $K^+K^-\pi^\pm$ as a function of $\phi^o\pi^\pm$ mass.

   b. Efficiency for having $p_{t\pi^\pm} > 900$ MeV/c as a function of $\phi^o\pi^\pm$ mass.

   c. Geometric efficiency as a function of $\phi^o\pi^\pm$ lab rapidity for $M = 2.0$ GeV/c^2

   d. Geometric efficiency as a function of $\phi^o\pi^\pm$ lab rapidity for $M = 5.0$ GeV/c^2.

3. (θ_x, θ_y) plots for $\pi^- p \to MX$ with $p_{tM} = \langle p_{tM} \rangle$. Decays $M \to \phi^o\pi^\pm$ and $\phi^o \to K^+K^-$ are shown for $\theta^* = 90^o$

   a. $M = 2.0$ GeV/c^2 b. $M = 5.0$ GeV/c^2

4. Kinematic distributions for $\pi^- p \to MX$, $M = 4$ GeV/c^2,

   a. $K^\pm$ lab polar angle

   b. K^+K^- opening angle

   c. Uncorrelated $\phi^o\pi^\pm$ inclusive mass distributions, all particles passing system apertures.

   d. $\phi^o\pi^\pm$ mass with $p_{t\pi} > 900$ Mev/C

5. Inclusive cross sections at 300 GeV/c vs composite mass assuming local quantum number compensation.

6. a. $(p_\gamma, \theta_\gamma)$ plot for $F^* \to F\gamma$ decay with $p_{tF}^* = 0$, $-y_F^* = 3.0$, $--y_F^* = 4.0$. Also indicated are the $\theta^* = 90^\circ$ points, $\odot$, and the MPS calorimeter apertures.

   b. $F\gamma$ mass resolution vs y_F^*. --- resolution due to dp_γ alone. - total resolution.

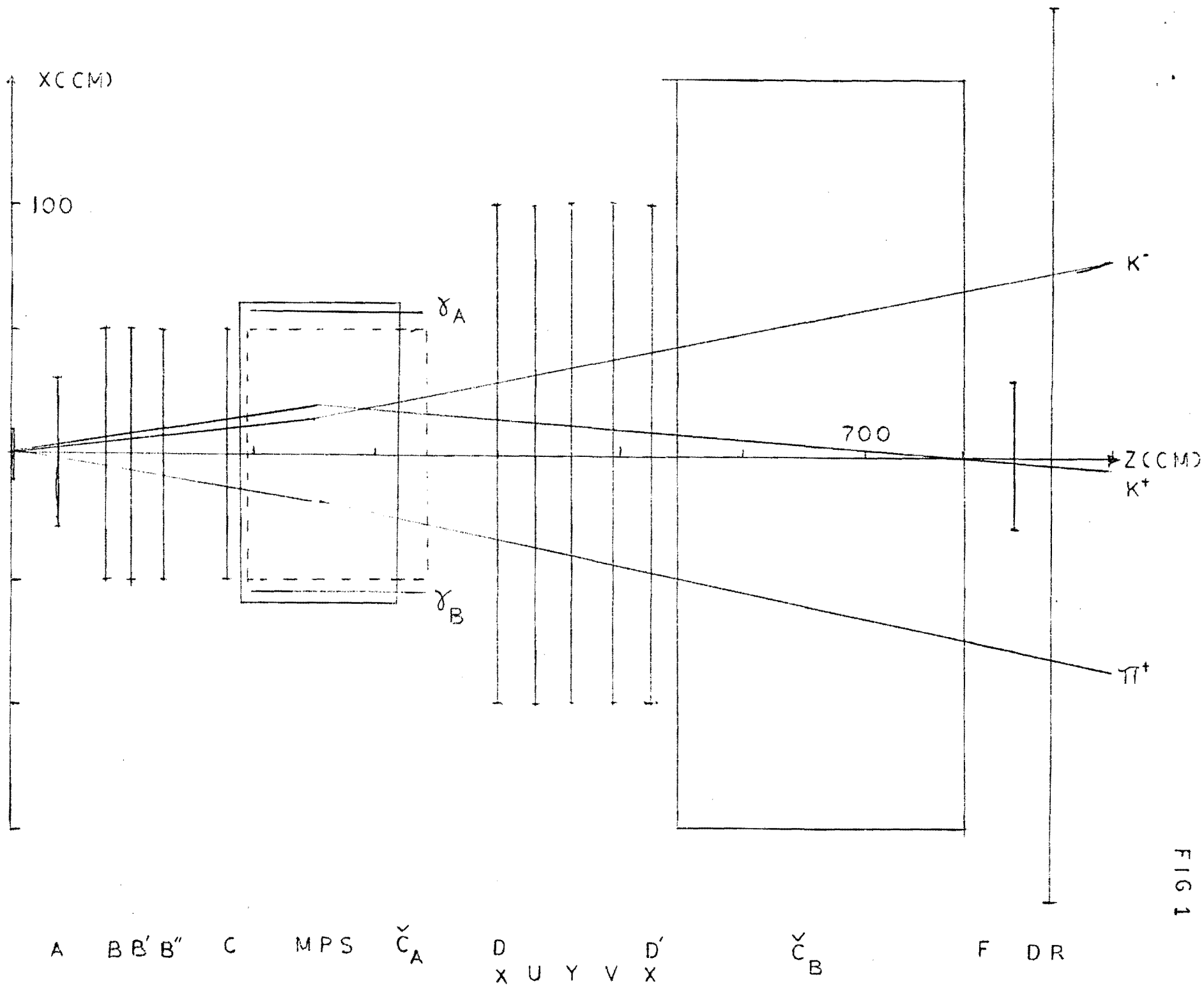
X(CM)
100
700
Z(CM)
K^-
K^+
π^+
γ_A
γ_B
A
B B' B''
C
M P S
$\check{C}_A$
D
X U Y V X
D'
$\check{C}_B$
F
D R

FIG 1

FIG 2

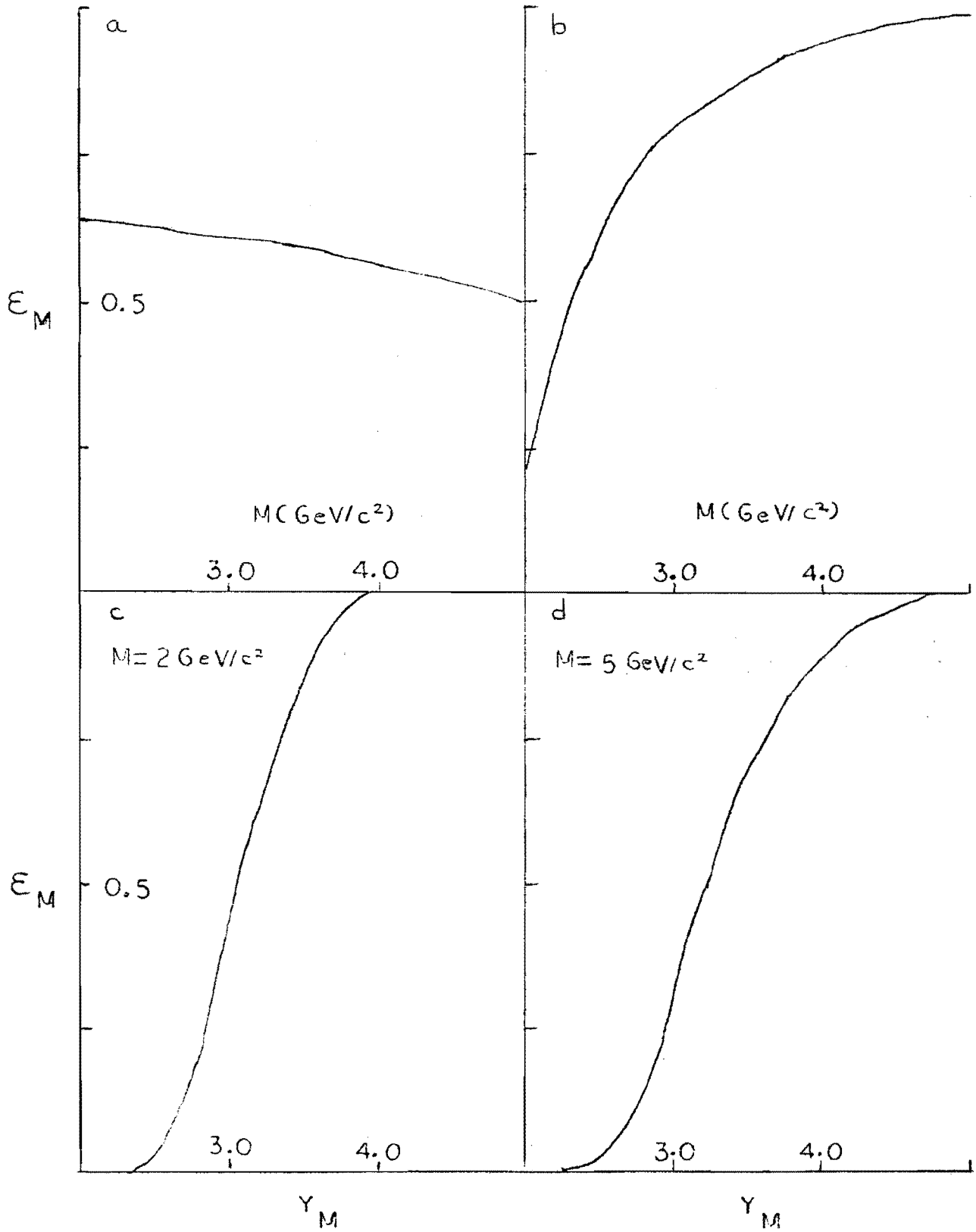

FIG 3

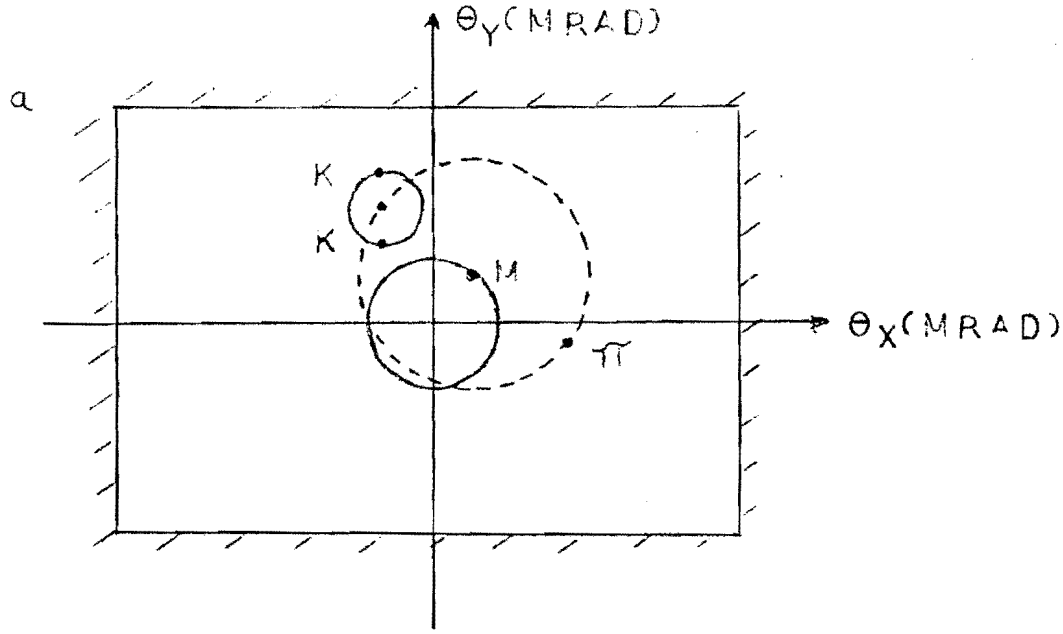
a
θ_Y(MRAD)
θ_X(MRAD)
K
K
M
π

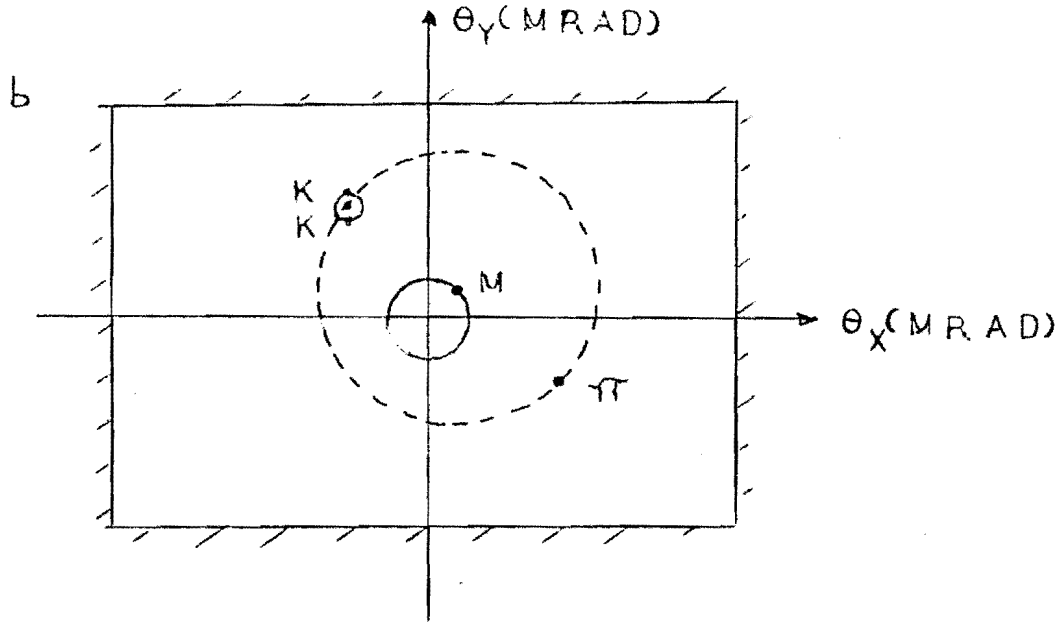
b
θ_Y(MRAD)
θ_X(MRAD)
K
K
M
π

FIG 4

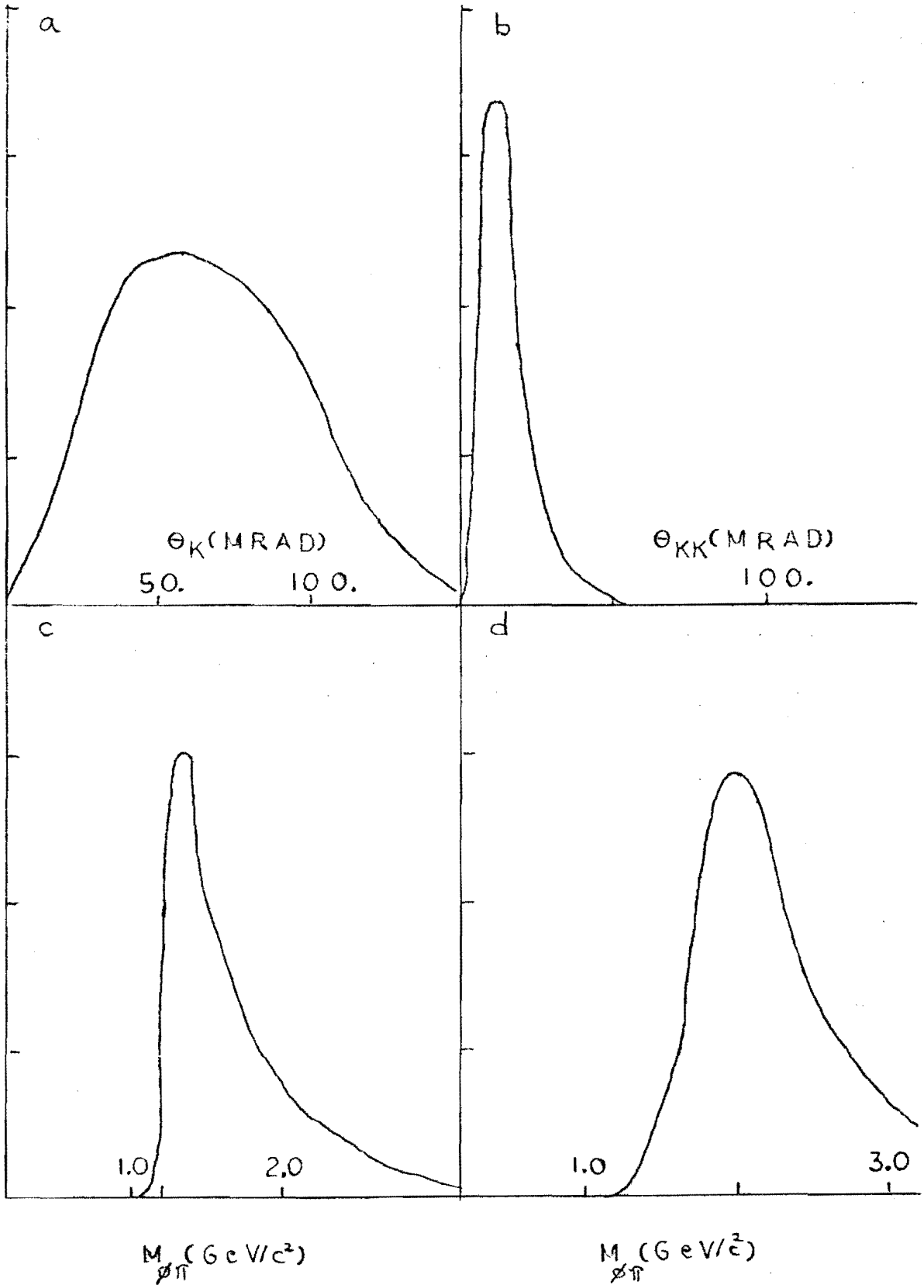
a
b
c
d
Θ_K (MRAD)
50.
100.
Θ_{KK} (MRAD)
100.
1.0
2.0
1.0
3.0
$M_{\phi\pi}$ (GeV/c²)
$M_{\phi\pi}$ (GeV/c²)

FIG 5

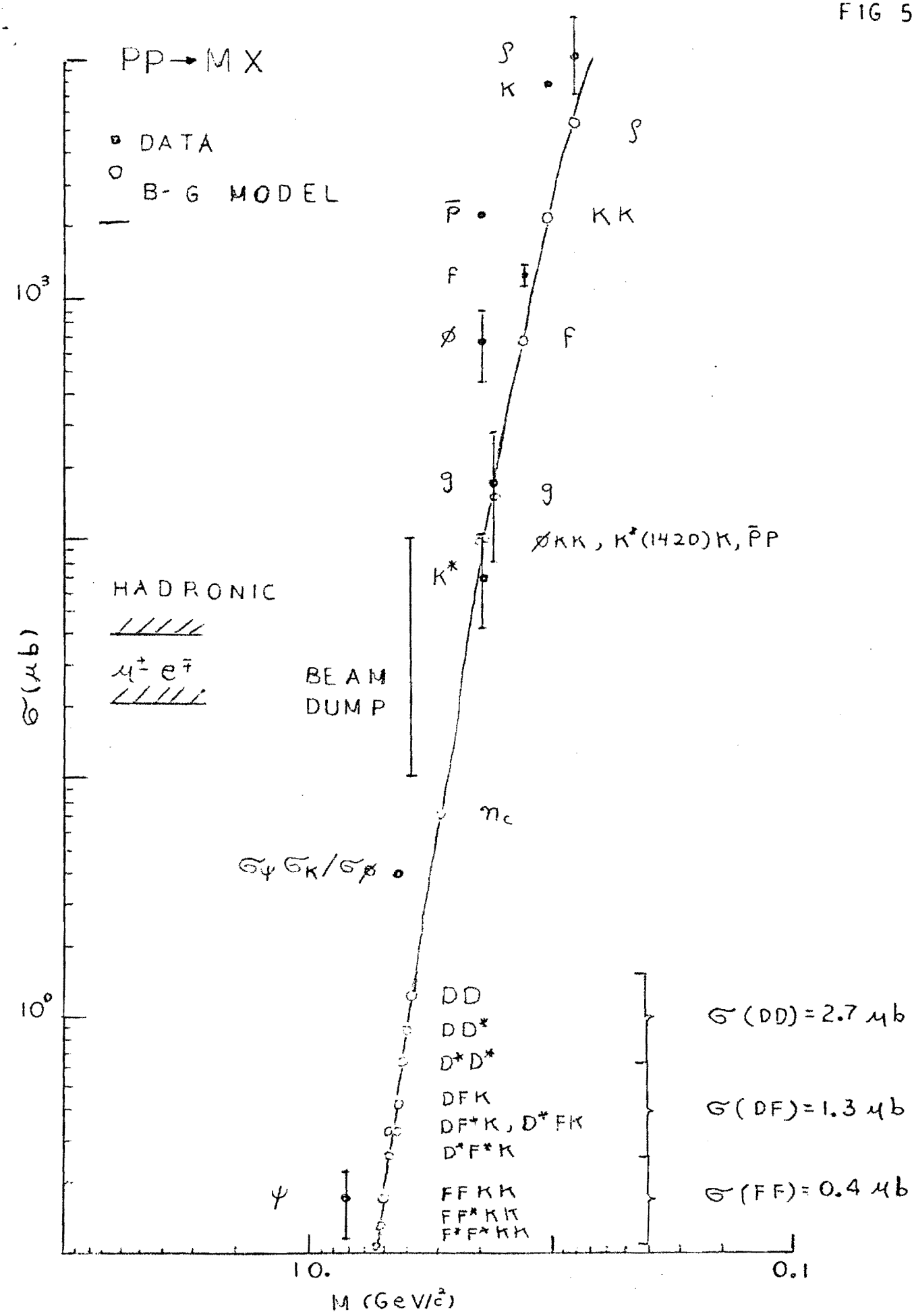
PP → MX
DATA
B-G MODEL
HADRONIC
μ± e∓
BEAM DUMP
ρ
K
ρ
P̄
KK
f
φ
f
g
g
φKK, K*(1420)K, P̄P
K*
η_c
σ_ψ σ_K/σ_φ
DD
DD*
D*D*
DFK
DF*K, D*FK
D*F*K
FFKK
FF*KK
F*F*KK
ψ
σ(DD) = 2.7 μb
σ(DF) = 1.3 μb
σ(FF) = 0.4 μb
10³
10⁰
σ (μb)
10.
0.1
M (GeV/c²)

FIG 6

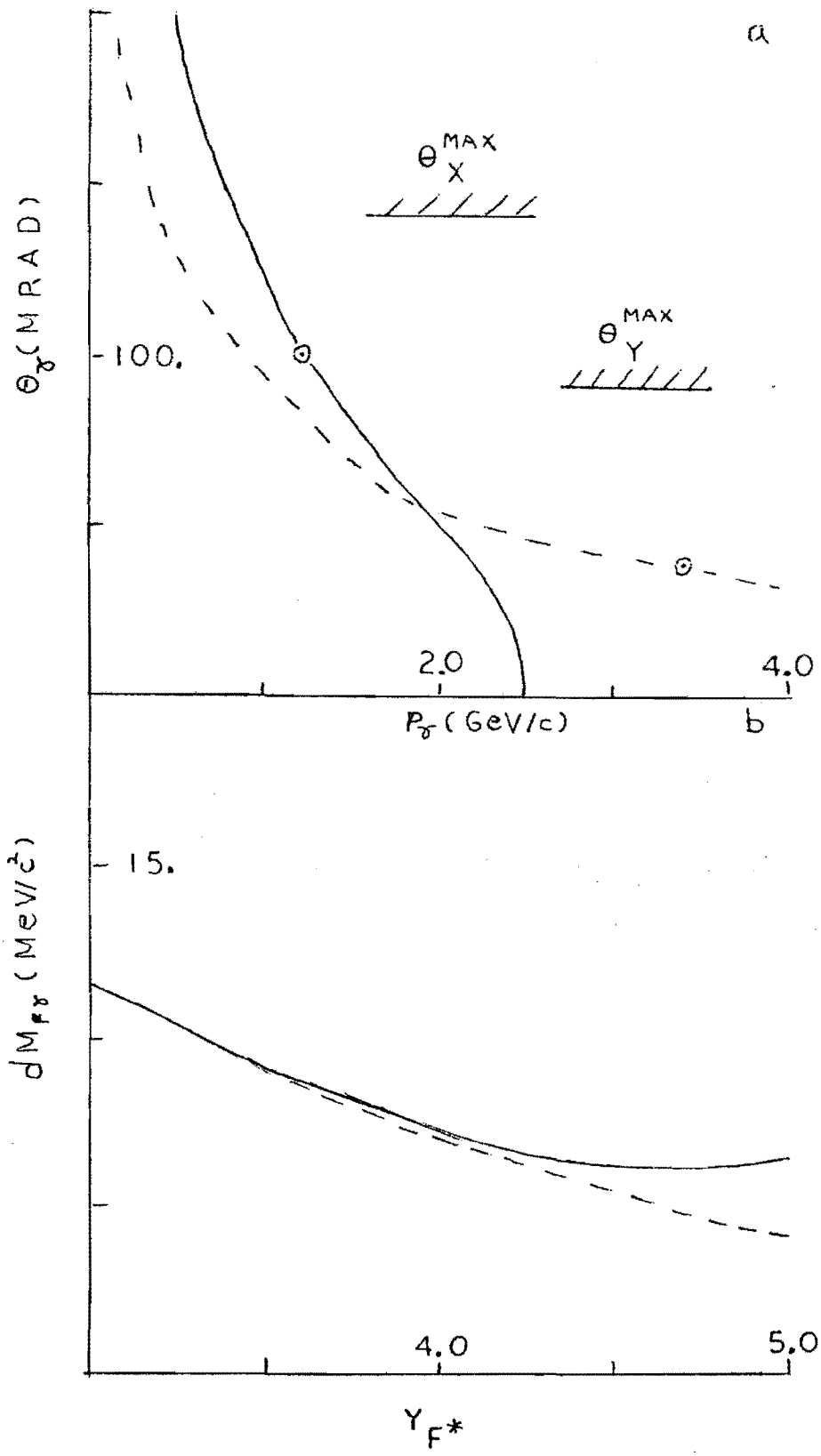
a
θ_X^{MAX}
θ_Y^{MAX}
θ_γ (MRAD)
100.
2.0
4.0
P_γ (GeV/c)
b
$dM_{F\gamma}$ (MeV/c²)
15.
4.0
5.0
Y_{F^*}